Pre-clinical evaluation of second generation PIM inhibitors for the treatment of T-cell acute lymphoblastic leukemia and lymphoma

Renate De Smedt,[1,2] Sofie Peirs,[1,2] Julie Morscio,[1,2] Filip Matthijssens,[1,2] Juliette Roels,[1,2,3] Lindy Reunes,[1,2] Beatrice Lintermans,[1,2] Steven Goossens,[1,2,4] Tim Lammens,[2,5] Nadine Van Roy,[1,2] Aurore Touzart,[6] Silvia Jenni,[7] Yi-Chien Tsai,[7] Federica Lovisa,[8] Lara Mussolin,[8] Valentina Serafin,[8] Filip Van Nieuwerburgh,[9] Dieter Deforce,[9] Anne Uyttebroeck,[10,11] Thomas Tousseyn,[12] Birgit Burkhardt,[13] Wolfram Klapper,[14] Barbara De Moerloose,[2,5] Yves Benoit,[2,5] Elizabeth Macintyre,[6] Jean-Pierre Bourquin,[7] Giuseppe Basso,[8] Benedetta Accordi,[8] Beat Bornhauser,[7] Jules Meijerink,[15] Peter Vandenberghe[16,17] and Pieter Van Vlierberghe[1,2]

[1]Department of Biomolecular Medicine, Ghent University, Belgium; [2]Cancer Research Institute Ghent (CRIG), Belgium; [3]Diagnostic Sciences, Ghent University, Belgium; [4]Molecular and Cellular Oncology Lab, Department for Biomedical Molecular Biology, Ghent University, Belgium; [5]Department of Pediatric Hematology-Oncology and Stem Cell Transplantation, Ghent University Hospital, Belgium; [6]Department of Hematology, APHP-Hôpital Necker, Paris, France; [7]Department of Oncology, and Children's Research Center, University Children's Hospital Zurich, Switzerland; [8]Department of Woman's and Child's Health, Hematology-Oncology Laboratory, Istituto di Ricerca Pediatrica (IRP) and University of Padova, Italy; [9]Laboratory of Pharmaceutical Biotechnology, Ghent University, Belgium; [10]Department of Pediatric Hematology-Oncology, University Hospitals Leuven, Belgium; [11]Department of Oncology, KU Leuven, Belgium; [12]Translational Cell and Tissue Research laboratory, KU Leuven, Belgium; [13]Department of Pediatric Hematology and Oncology, University of Münster, Germany; [14]Department of Pathology, Hematopathology Section, UKSH Campus Kiel, Germany; [15]The Princess Máxima Center for Pediatric Oncology, Utrecht, the Netherlands; [16]Department of Hematology, University Hospitals Leuven, Belgium and [17]Center for Human Genetics, KU Leuven, Belgium

Correspondence: pieter.vanvlierberghe@ugent.be
doi:10.3324/haematol.2018.199257

Supplementary Legends

Table S1. Exome sequencing of t(6;7) TCRβ-PIM1 TLX1^{+} PIM1^{high} T-LBL patient. Bone marrow DNA was used as control (case with no bone marrow infiltration). Unique variants in pleural effusion are listed.

Table S2. PIM1 correlation in *LYL1*$^{+}$, *TLX1*$^{+}$, *TLX3*$^{+}$ and *HOXA*$^{+}$ T-ALLs (n=39). Top 100 positively correlated genes with PIM1 in T-ALL cohort (n=39) listed with the Pearson correlation coefficient r.

Table S3. Geneset enrichment analysis (GSEA) of TP-3654 treated PDX splenocytes. Patient derived xenograft (PDX) splenocytes were treated with TP-3654 for 24h and subsequently collected for RNA sequencing. The table shows GSEA analysis of geneset collections h.all.v6.1.symbols.gmt [Hallmarks] and c2.all.v6.1.symbols.gmt [Curated], for responder patients (TLX3^{+} PHF6^{mut} NOTCH1^{mut} T-ALL and TLX1^{+} TCRβ-PIM1 NOTCH1^{mut} T-LBL). Biologically relevant genesets are shown (FDR < 0.25).

Figure S1. A t(6;7)(p21;q34) translocation causing PIM1 oncogene upregulation in a T-LBL case.
(A) TLA of a T-LBL case with TCRβ (7q34) as viewpoint. Additional reads were detected at 6p21.2, suggesting the presence of a t(6;7) translocation. The genomic breakpoint of this rearrangement is situated 133kb upstream of the PIM1 kinase. The exact breakpoint sequence is shown. (B) Schematic overview of the t(6;7)(p21;q34) translocation as identified in a case of pediatric T-LBL. (C) Quantitative RT-PCR showing PIM1 expression levels in normal CD34+ T-cells and the t(6;7)(p21;q34)-positive T-LBL patient. HMBS, TBP and HPRT1 were used as reference genes. CNRQ = calibrated normal relative quantities (D) Sanger sequencing analysis of a single nucleotide polymorphism at genomic DNA and corresponding cDNA level uncovers skewed allelic PIM1 expression in the t(6;7)(p21;q34)-positive T-LBL patient. (E) Quantitative RT-PCR showing *TLX1* expression levels in the t(6;7)(p21;q34)-positive T-LBL patient and the *TLX1+* T-ALL cell line ALL-SIL. HMBS, TBP and HPRT1 were used as reference genes. CNRQ = calibrated normal relative quantities

Figure S2. Array CGH of the t(6;7) TCRβ-PIM1 *TLX1*$^{+}$ PIM1^{high} T-LBL patient. Sample 1 is pleural effusion from the TCRβ-PIM1 T-LBL patient. Sample 2 is bone marrow DNA and is used as a control (T-LBL case with no bone marrow infiltration). Red bars depict losses whereas blue bars are gains.

Figure S3. PIM1 expression in primary T-ALL and T-LBL. (A) PIM1 expression analysis based on microarray data in molecular genetic subgroups of human T-ALL and subsets of normal human T-precursor cells (n=64). * = p < 0.05 (B) Positive correlation between PIM1 mRNA expression and JAK-STAT pathway members CISH and STAT4 in *LYL1*$^{+}$, *TLX1*$^{+}$, *TLX3*$^{+}$ and *HOXA*$^{+}$ T-ALLs (n=39). (C) PIM1 qPCR data from ruxolitinib treated DND-41 cells (400 nM for 6h). HMBS, TBP and HPRT1 were used as reference genes. (D) PIM1 expression analysis in IL7R/JAK1/JAK3 mutants compared to wildtype patients in a second independent T-ALL cohort (n=117) (E) Relative *PIM1* expression (log2) from microarray data of that same T-ALL cohort (n=117). High *PIM1* levels are seen in immature and *TLX*$^{+}$ subtypes, whereas proliferative (*NKX2-1*$^{+}$) and TAL1/LMO2 rearranged T-ALLs show low *PIM1* expression levels. * = p < 0.05 (F) *PIM1* qPCR analysis of primary T-LBL (n=79) and T-ALL (n=21) patient specimens. *PIM1* expression levels are normalized to *ABL1* expression. n.s. = not significant (G) *PIM1* qPCR analysis of a second independent T-LBL cohort (n=30). *PIM1* expression levels are normalized to *GAPDH* expression. TCRβ-PIM1^{+} T-LBL patient is visualized in red.

Figure S4. (A) Break-apart FISH analysis using probes flanking the genomic breakpoint on 6p21 on PDX TCRβ-PIM1 T-LBL spleen cells. (B) *PIM1* qPCR data of TCRβ-PIM1 T-LBL cells from the primary patient compared to spleen cells from the PDX model. HMBS, TBP and HPRT1 were used as reference genes. CNRQ = calibrated normal relative quantities (C) *PIM1* qPCR of a TLX3^{+} PHF6^{mut} NOTCH1^{mut} T-ALL and a SIL-TAL1 FBXW7^{mut} NOTCH1^{mut} T-ALL case. HMBS, TBP and HPRT1 were used as reference genes. CNRQ = calibrated normal relative quantities (D) *PIM1* western blot analysis of a TLX3^{+} PHF6^{mut} NOTCH1^{mut} T-ALL and a SIL-TAL1 FBXW7^{mut} NOTCH1^{mut} T-ALL case.

Figure S5. PIM1, PIM2 and PIM3 DESeq2 normalized counts from RNASeq data from PDX spleen cells of the TLX1^{+} TCRβ-PIM1 T-LBL case the TLX3^{+} PHF6^{mut} NOTCH1^{mut} T-ALL and thea SIL-TAL1 FBXW7^{mut} NOTCH1^{mut} T-ALL case.

Figure S6. Schematic representation of experimental strategy for RNA sequencing analysis of primary xenograft cells upon PIM1 inhibition by 1μM TP-3654 after 24 hours.

Figure S7. Gene Set Enrichment Analysis plots for down- and upregulated genesets after PIM1 inhibition in PIM1i responder patients (TLX^{+}). GSEA revealed that genes significantly downregulated upon PIM1 inhibition were enriched for gene sets related to amino acid deprivation, while genes significantly upregulated upon PIM1 inhibition were involved in cell cycle regulation and included gene sets associated with G2/M cell cycle transition and E2F3 target genes. NES = Normalized Enrichment Score

Figure S8. (A) Western blot analysis of MCL1 protein levels in *ex vivo* treated xenograft spleen cells obtained from TCRβ-PIM1^{+} T-LBL, TLX3^{+} PIM1^{high} T-ALL and SIL-TAL1^{+} PIM1^{low} T-ALL patients treated with PIM1 inhibitor TP-3654 (1μM, 24h). (B) Cell viability curves of an 72h *ex vivo* combination treatment of PIM1 inhibitors TP-3654 and AZD1208 with the BCL2 inhibitor ABT-199 on TCRβ-PIM1 T-LBL PDX spleen cells. The combination index (CI) shown represents the average of the CIs at the ED50, ED75, and ED90 effect levels for each experiment. 0.9 , CI , 1.1: nearly additive; 0.85 , CI , 0.9: slight synergism; 0.7 , CI , 0.85: moderate synergism; 0.3 , CI , 0.7: synergism; 0.1 , CI , 0.3: strong synergism

Figure S9. Combination treatment of with PIM1 inhibitors and dexamethasone for 72h on *ex vivo* co-culture system on TCRβ-PIM1 TLX1^{+} PIM1^{high} T-LBL cells. (A) Cell viability curves of an 72h *ex vivo* combination treatment of PIM1 inhibitors TP-3654 and AZD1208 with the glucocorticoid dexamethasone on TCRβ-PIM1 T-LBL PDX spleen cells. (B) Interaction landscapes for combination treatment are shown, using a Zero Interaction Potency (ZIP, https://synergyfinder.fimm.fi/, Yadav et al., *Computational and structural biotechnology journal*, 2018) model. Delta scores of zero imply probabilistic independence and dose additivity, whereas positive delta scores (depicted in red) imply synergism. At the most synergistic area (depicted by the white rectangle), we see on average 20% more cell inhibition compared to the expected effect with monotherapy.

Table S1. Exome sequencing of t(6;7) TCRβ-PIM1 TLX1^{+} PIM1^{high} T-LBL patient.

	Unique variants pleural effusion INDEL
1	AGAP9:NM_001190810:exon8:c.736delC:p.L246fs
2	ANKRD36B:NM_025190:exon39:c.3250_3251del:p.H1084fs
3	BTBD2:NM_017797:exon1:c.160_162del:p.54_54del
4	CNTNAP3:NM_033655:exon10:c.1599delG:p.A533fs
5	**EP300**:NM_001429:exon21:c.3728dupT:p.L1243fs
6	FAM104B:NM_001166699:exon3:c.179delC:p.A60fs
7	FAM46A:NM_017633:exon2:c.131_132insCGGCGACTTCGGCGGCGGCGACTTCGGCGGCGGC GACTTCGGCGG:p.G44delinsGGDFGGGDFGGGDFGG
8	HLA-DRB5:NM_002125:exon3:c.371_373del:p.124_125del
9	**IKZF1**:NM_001220765:exon7:c.725_745del:p.242_249del
10	MICALCL:NM_032867:exon3:c.1366_1367insCTCCTCCTC:p.A456delinsAPPP
11	NBPF14:NM_015383:exon65:c.8168_8169insGAG:p.R2723delinsRR
12	**NOTCH1**:NM_017617:exon34:c.7476_7477insTAAGGG:p.P2493delinsX
13	NPIPB11:NM_001310137:exon7:c.1127_1252del:p.376_418del
14	PABPC3:NM_030979:exon1:c.465_466insG:p.I155fs
15	TRAK1:NM_001265608:exon14:c.2063_2064insGGAGGAGGA:p.T688delinsTEEE
16	TXNDC11:NM_001303447:exon9:c.1689_1690insTCATCGCAACC:p.L564fs
17	VEZF1:NM_007146:exon5:c.1046_1047insGCA:p.Q349delinsQQ
18	ZBTB10:NM_001105539:exon2:c.1071_1072insCGA:p.Q357delinsQR

Table S2. PIM1 correlation in *LYL1*$^{+}$, *TLX1*$^{+}$, *TLX3*$^{+}$ and *HOXA*$^{+}$ T-ALLs (n=39).

	Probe	**Gene**	**r (pearson correlation coefficient)**
1	X209193_at	**PIM1**	1
2	X223961_s_at	**CISH**	0.845204398203216
3	X206118_at	**STAT4**	0.843934618961696
4	X223377_x_at	**CISH**	0.837713567123651
5	X221223_x_at	**CISH**	0.815041404756306
6	X213400_s_at	**TBL1X**	0.705309270375358
7	X201204_s_at	**RRBP1**	0.698391240981059
8	X201206_s_at	**RRBP1**	0.68969052197247
9	X1552788_a_at	**HELB**	0.683845995815829
10	X203372_s_at	**SOCS2**	0.683630480353313
11	X201868_s_at	**TBL1X**	0.683000585570833
12	X201203_s_at	**RRBP1**	0.682237199902737
13	X209115_at	**UBE1C**	0.68220999922514
14	X1552787_at	**HELB**	0.681501555677976
15	X1555600_s_at	**APOL4**	0.674232679581437
16	X205480_s_at	**UGP2**	0.672390660779372
17	X204918_s_at	**MLLT3**	0.671469392289337
18	X200761_s_at	**ARL6IP5**	0.671422054654829
19	X201170_s_at	**BHLHB2**	0.670436300203455
20	X209879_at	**SELPLG**	0.668947354126419

21	X201328_at	**ETS2**	0.668139119432817
22	X203373_at	**SOCS2**	0.665456133414931
23	X228000_at	**ADC**	0.654715488223528
24	X201867_s_at	**TBL1X**	0.652282020344968
25	X204917_s_at	**MLLT3**	0.649722049326464
26	X200760_s_at	**ARL6IP5**	0.649038330200558
27	X201869_s_at	**TBL1X**	0.648864914440236
28	X218845_at	**DUSP22**	0.645556910248701
29	X230170_at	**OSM**	0.645048372418293
30	X235046_at	**---**	0.64310319054216
31	X202688_at	**TNFSF10**	0.639936679931677
32	X225093_at	**UTRN**	0.637853689520773
33	X210001_s_at	**SOCS1**	0.637726084811546
34	X205376_at	**INPP4B**	0.635679859293135
35	X209880_s_at	**SELPLG**	0.631252547494127
36	X209475_at	**USP15**	0.630082855035799
37	X229511_at	**SMARCE1**	0.627452081629699
38	X202687_s_at	**TNFSF10**	0.626926705758203
39	X240064_at	**---**	0.626350102680814
40	X237837_at	**BCL2**	0.625625083913538
41	X229057_at	**SCN2A2**	0.622899223804802
42	X202124_s_at	**TRAK2**	0.622071466864777
43	X211434_s_at	**CCRL2 /// LOC642312**	0.619727400084829
44	X229373_at	**---**	0.618986731379375
45	X231241_at	**SLFN5**	0.618082774299647
46	X231698_at	**LOC647115**	0.616481189857467
47	X1559315_s_at	**LOC144481**	0.615207765488568
48	X236692_at	**---**	0.614919072458742
49	X1567013_at	**NFE2L2**	0.614877320706445
50	X202125_s_at	**TRAK2**	0.614827055231061
51	X215388_s_at	**CFH /// CFHR1**	0.614652769899531
52	X213800_at	**CFH**	0.613482016688848
53	X213261_at	**LBA1**	0.612970566108157
54	X203445_s_at	**CTDSP2**	0.609984634562435
55	X217599_s_at	**MDFIC**	0.60942274472097
56	X213024_at	**TMF1**	0.608874204289458
57	X214329_x_at	**TNFSF10**	0.608450521016795
58	X203989_x_at	**F2R**	0.606615867342229
59	X1553815_a_at	**MGC17403**	0.605568115546061
60	X240232_at	**C3ORF1**	0.605454514237657
61	X236935_at	**---**	0.605021658646707
62	X219125_s_at	**RAG1AP1**	0.604434282106758
63	X227686_at	**OXNAD1**	0.599573001523555
64	X211675_s_at	**MDFIC**	0.598657445602537
65	X224929_at	**LOC340061**	0.598510920922731
66	X206073_at	**COLQ**	0.59807265248446
67	X224916_at	**LOC340061**	0.597000900617519
68	X213309_at	**PLCL2**	0.596061039477732
69	X232539_at	**---**	0.595544169269788

70	X201169_s_at	**BHLHB2**	0.595183853651702
71	X231832_at	**GALNT4**	0.594677008034422
72	X207334_s_at	**TGFBR2**	0.593880588786951
73	X223611_s_at	**LNX1**	0.593590354823471
74	X235777_at	**ANKRD44**	0.592877381006413
75	X213351_s_at	**TMCC1**	0.58945954889359
76	X237875_at	**STK10**	0.588306895422471
77	X206011_at	**CASP1**	0.588014787132169
78	X244028_at	**USP15**	0.587882388037
79	X201243_s_at	**ATP1B1**	0.587016440128148
80	X226702_at	**LOC129607**	0.585465072845878
81	X231968_at	**---**	0.585427214164608
82	X200649_at	**NUCB1**	0.585334652505354
83	X219885_at	**SLFN12**	0.584866382145803
84	X201146_at	**NFE2L2**	0.58474557215436
85	X228394_at	**---**	0.583933659431994
86	X218870_at	**ARHGAP15**	0.58296967185708
87	X231960_at	**BRWD1**	0.581228213805855
88	X218632_at	**HECTD3**	0.579455934367618
89	X219279_at	**DOCK10**	0.579285862176833
90	X202763_at	**CASP3**	0.578061820222281
91	X240175_at	**---**	0.577716532058264
92	X213401_s_at	**TBL1X**	0.577360274041345
93	X226853_at	**BMP2K**	0.57532132238489
94	X211368_s_at	**CASP1**	0.57384500662817
95	X209941_at	**RIPK1**	0.573338197086031
96	X226048_at	**MAPK8**	0.572905300948148
97	X226440_at	**DUSP22**	0.571747773784722
98	X203732_at	**TRIP4**	0.569390956673752
99	X218928_s_at	**SLC37A1**	0.568617337381424
100	X209970_x_at	**CASP1**	0.567475553514649

Table S3. Geneset enrichment analysis (GSEA) of TP-3654 treated PDX splenocytes.

HALLMARK_UP after TP-3654

	GS	**SIZE**	**ES**	**NES**	**NOM p-val**	**FDR q-val**	**FWER p-val**	**RANK AT MAX**	**LEADING EDGE**
1	HALLMARK_MITOTIC_SPINDLE	176	0.21	3.22	0.000	0.000	0.000	6287	tags=80%, list=60%, signal=195%
2	HALLMARK_E2F_TARGETS	193	0.17	2.84	0.000	0.000	0.000	834	tags=25%, list=8%, signal=27%
3	HALLMARK_G2M_CHECKPOINT	185	0.17	2.58	0.000	0.000	0.002	1589	tags=31%, list=15%, signal=36%

4	HALLMARK_SPERMATOGENESIS	57	0.22	1.97	0.004	0.028	0.136	2837	tags=49%, list=27%, signal=67%
5	HALLMARK_TNFA_SIGNALING_VIA_NFKB	128	0.14	1.82	0.006	0.052	0.288	7293	tags=83%, list=69%, signal=266%
6	HALLMARK_KRAS_SIGNALING_UP	89	0.16	1.75	0.021	0.062	0.386	4765	tags=61%, list=45%, signal=110%
7	HALLMARK_UV_RESPONSE_DN	97	0.15	1.69	0.025	0.075	0.508	6952	tags=80%, list=66%, signal=234%
8	HALLMARK_EPITHELIAL_MESENCHYMAL_TRANSITION	73	0.17	1.67	0.021	0.073	0.549	7069	tags=84%, list=67%, signal=252%
9	HALLMARK_APICAL_SURFACE	20	0.27	1.45	0.090	0.176	0.877	7182	tags=95%, list=68%, signal=298%

HALLMARK_DOWN after TP-3654

	GS	SIZE	ES	NES	NOM p-val	FDR q-val	FWER p-val	RANK AT MAX	LEADING EDGE
1	HALLMARK_MYC_TARGETS_V1	191	-0.43	-6.70	0.000	0.000	0.000	2552	tags=66%, list=24%, signal=85%
2	HALLMARK_MTORC1_SIGNALING	184	-0.37	-5.73	0.000	0.000	0.000	1701	tags=52%, list=16%, signal=61%
3	HALLMARK_OXIDATIVE_PHOSPHORYLATION	186	-0.33	-5.10	0.000	0.000	0.000	2846	tags=59%, list=27%, signal=80%
4	HALLMARK_MYC_TARGETS_V2	52	-0.58	-4.91	0.000	0.000	0.000	2647	tags=83%, list=25%, signal=110%
5	HALLMARK_ADIPOGENESIS	146	-0.26	-3.70	0.000	0.000	0.000	2894	tags=53%, list=27%, signal=73%
6	HALLMARK_CHOLESTEROL_HOMEOSTASIS	49	-0.39	-3.34	0.000	0.000	0.000	2349	tags=61%, list=22%, signal=78%
7	HALLMARK_UNFOLDED_PROTEIN_RESPONSE	101	-0.27	-3.04	0.000	0.000	0.000	2749	tags=52%, list=26%, signal=70%
8	HALLMARK_FATTY_ACID_METABOLISM	112	-0.25	-3.00	0.000	0.000	0.000	2144	tags=45%, list=20%, signal=55%
9	HALLMARK_GLYCOLYSIS	131	-0.21	-2.84	0.000	0.000	0.000	4968	tags=68%, list=47%, signal=127%
10	HALLMARK_UV_RESPONSE_UP	104	-0.21	-2.47	0.000	0.001	0.006	4239	tags=61%, list=40%, signal=100%
11	HALLMARK_IL2_STAT5_SIGNALING	133	-0.17	-2.32	0.002	0.001	0.013	5106	tags=65%, list=48%,

									signal=125%
12	HALLMARK_PEROXISOME	72	-0.22	-2.24	0.002	0.003	0.028	2349	tags=44%, list=22%, signal=57%
13	HALLMARK_INTERFERON_GAMMA_RESPONSE	142	-0.15	-2.04	0.002	0.010	0.096	3734	tags=50%, list=35%, signal=76%
14	HALLMARK_XENOBIOTIC_METABOLISM	99	-0.17	-1.99	0.006	0.012	0.126	4097	tags=56%, list=39%, signal=90%
15	HALLMARK_IL6_JAK_STAT3_SIGNALING	49	-0.23	-1.90	0.015	0.018	0.185	6600	tags=86%, list=63%, signal=229%
16	HALLMARK_REACTIVE_OXIGEN_SPECIES_PATHWAY	41	-0.24	-1.88	0.008	0.019	0.207	2846	tags=51%, list=27%, signal=70%
17	HALLMARK_ANDROGEN_RESPONSE	78	-0.14	-1.47	0.085	0.137	0.845	824	tags=22%, list=8%, signal=23%
18	HALLMARK_INTERFERON_ALPHA_RESPONSE	77	-0.14	-1.38	0.118	0.188	0.950	3239	tags=44%, list=31%, signal=63%
19	HALLMARK_DNA_REPAIR	128	-0.10	-1.34	0.118	0.208	0.970	2228	tags=31%, list=21%, signal=39%

ALL_UP after TP-3654_top 50

	GS	SIZE	ES	NES	NOM p-val	FDR q-val	FWER p-val	RANK AT MAX	LEADING EDGE
1	FISCHER_G2_M_CELL_CYCLE	199	0.35	5.64	0.000	0.000	0.000	1644	tags=50%, list=16%, signal=58%
2	ROSTY_CERVICAL_CANCER_PROLIFERATION_CLUSTER	125	0.39	5.04	0.000	0.000	0.000	1782	tags=55%, list=17%, signal=66%
3	WANG_RESPONSE_TO_GSK3_INHIBITOR_SB216763_UP	262	0.26	4.93	0.000	0.000	0.000	2667	tags=51%, list=25%, signal=66%
4	KONG_E2F3_TARGETS	85	0.45	4.78	0.000	0.000	0.000	3013	tags=73%, list=29%, signal=101%
5	CHANG_CYCLING_GENES	131	0.35	4.56	0.000	0.000	0.000	2479	tags=58%, list=24%, signal=75%
6	GOBERT_OLIGODENDROCYTE_DIFFERENTIATION_UP	453	0.18	4.46	0.000	0.000	0.000	1579	tags=33%, list=15%, signal=37%
7	WHITFIELD_CELL_CYCLE_G2	142	0.32	4.40	0.000	0.000	0.000	1979	tags=50%, list=19%, signal=61%
8	DUTERTRE_ESTRADIOL_RESPONSE_24HR_UP	260	0.23	4.32	0.000	0.000	0.000	1562	tags=38%, list=15%, signal=43%
9	LEE_EARLY_T_LYMPH	97	0.36	4.18	0.000	0.000	0.000	1562	tags=51%,

	OCYTE_UP								list=15%, signal=59%
10	SHEPARD_CRUSH_AND_BURN_MUTANT_DN	109	0.33	4.06	0.000	0.000	0.000	2801	tags=60%, list=27%, signal=80%
11	REACTOME_PEPTIDE_CHAIN_ELONGATION	83	0.38	4.01	0.000	0.000	0.000	4694	tags=82%, list=45%, signal=147%
12	ZHAN_MULTIPLE_MYELOMA_PR_UP	40	0.53	3.95	0.000	0.000	0.000	1579	tags=68%, list=15%, signal=79%
13	KEGG_RIBOSOME	84	0.36	3.94	0.000	0.000	0.000	2611	tags=61%, list=25%, signal=80%
14	ODONNELL_TFRC_TARGETS_DN	98	0.34	3.90	0.000	0.000	0.000	2597	tags=58%, list=25%, signal=76%
15	KANG_DOXORUBICIN_RESISTANCE_UP	49	0.46	3.90	0.000	0.000	0.000	2479	tags=69%, list=24%, signal=90%
16	WHITFIELD_CELL_CYCLE_S	121	0.30	3.84	0.000	0.000	0.000	4563	tags=73%, list=43%, signal=127%
17	TANG_SENESCENCE_TP53_TARGETS_DN	46	0.47	3.74	0.000	0.000	0.000	1744	tags=63%, list=17%, signal=75%
18	REACTOME_3_UTR_MEDIATED_TRANSLATIONAL_REGULATION	102	0.31	3.71	0.000	0.000	0.000	2611	tags=56%, list=25%, signal=74%
19	AMUNDSON_GAMMA_RADIATION_RESPONSE	37	0.51	3.70	0.000	0.000	0.000	2056	tags=70%, list=20%, signal=87%
20	ZWANG_DOWN_BY_2ND_EGF_PULSE	152	0.26	3.64	0.000	0.000	0.000	2882	tags=53%, list=27%, signal=71%
21	CHIANG_LIVER_CANCER_SUBCLASS_PROLIFERATION_UP	129	0.28	3.64	0.000	0.000	0.000	1653	tags=43%, list=16%, signal=51%
22	KOBAYASHI_EGFR_SIGNALING_24HR_DN	202	0.22	3.53	0.000	0.000	0.000	2065	tags=41%, list=20%, signal=50%
23	NAKAYAMA_SOFT_TISSUE_TUMORS_PCA2_UP	51	0.40	3.44	0.000	0.000	0.000	1755	tags=57%, list=17%, signal=68%
24	SHEPARD_BMYB_TARGETS	42	0.45	3.43	0.000	0.000	0.000	1755	tags=62%, list=17%, signal=74%
25	SOTIRIOU_BREAST_CANCER_GRADE_1_VS_3_UP	135	0.24	3.39	0.000	0.000	0.000	2065	tags=44%, list=20%, signal=54%
26	REACTOME_NONSENSE_MEDIATED_DECAY_ENHANCED_BY_THE_EXON_JUNCTION_COMPLEX	103	0.28	3.33	0.000	0.000	0.000	3623	tags=62%, list=34%, signal=94%

27	REACTOME_INFLUENZA_VIRAL_RNA_TRANSCRIPTION_AND_REPLICATION	98	0.29	3.31	0.000	0.000	0.001	2611	tags=53%, list=25%, signal=70%
28	HADDAD_B_LYMPHOCYTE_PROGENITOR	210	0.20	3.30	0.000	0.000	0.001	5387	tags=70%, list=51%, signal=141%
29	BILANGES_SERUM_AND_RAPAMYCIN_SENSITIVE_GENES	60	0.36	3.27	0.000	0.000	0.001	4822	tags=82%, list=46%, signal=150%
30	PUJANA_BRCA2_PCC_NETWORK	396	0.14	3.26	0.000	0.000	0.002	1835	tags=31%, list=17%, signal=36%
31	WHITEFORD_PEDIATRIC_CANCER_MARKERS	104	0.28	3.24	0.000	0.000	0.002	1990	tags=46%, list=19%, signal=56%
32	GREENBAUM_E2A_TARGETS_UP	27	0.51	3.21	0.000	0.000	0.002	1688	tags=67%, list=16%, signal=79%
33	REICHERT_MITOSIS_LIN9_TARGETS	25	0.53	3.20	0.000	0.000	0.002	2056	tags=72%, list=20%, signal=89%
34	BENPORATH_ES_WITH_H3K27ME3	253	0.17	3.19	0.000	0.000	0.002	7812	tags=91%, list=74%, signal=344%
35	ZHOU_CELL_CYCLE_GENES_IN_IR_RESPONSE_24HR	106	0.26	3.18	0.000	0.000	0.002	1782	tags=42%, list=17%, signal=51%
36	WU_APOPTOSIS_BY_CDKN1A_VIA_TP53	48	0.38	3.12	0.000	0.000	0.002	5045	tags=85%, list=48%, signal=163%
37	PYEON_HPV_POSITIVE_TUMORS_UP	73	0.30	3.00	0.000	0.000	0.003	2819	tags=56%, list=27%, signal=76%
38	GOZGIT_ESR1_TARGETS_DN	346	0.14	2.98	0.000	0.000	0.005	7982	tags=89%, list=76%, signal=357%
39	CROONQUIST_IL6_DEPRIVATION_DN	91	0.26	2.94	0.000	0.000	0.005	3067	tags=55%, list=29%, signal=77%
40	PUJANA_XPRSS_INT_NETWORK	159	0.20	2.92	0.000	0.000	0.007	3038	tags=48%, list=29%, signal=67%
41	REACTOME_CELL_CYCLE	335	0.14	2.91	0.000	0.000	0.008	1089	tags=24%, list=10%, signal=26%
42	BURTON_ADIPOGENESIS_3	89	0.25	2.90	0.000	0.000	0.010	1835	tags=43%, list=17%, signal=51%
43	FARMER_BREAST_CANCER_CLUSTER_2	30	0.44	2.90	0.000	0.000	0.010	1998	tags=63%, list=19%, signal=78%
44	REACTOME_SRP_DEPENDENT_COTRANSLATIONAL_PROTEIN_TARGETING_TO_MEMB	105	0.24	2.88	0.000	0.000	0.011	2611	tags=49%, list=25%, signal=64%

	RANE								
45	CHNG_MULTIPLE_MYELOMA_HYPERPLOID_UP	49	0.35	2.88	0.000	0.000	0.011	4272	tags=76%, list=41%, signal=126%
46	KINSEY_TARGETS_OF_EWSR1_FLII_FUSION_DN	181	0.18	2.87	0.000	0.000	0.011	4064	tags=56%, list=39%, signal=90%
47	KIM_WT1_TARGETS_DN	366	0.13	2.86	0.000	0.000	0.012	3613	tags=47%, list=34%, signal=69%
48	ZHANG_TLX_TARGETS_36HR_DN	175	0.19	2.86	0.000	0.000	0.012	2054	tags=38%, list=20%, signal=46%
49	CROONQUIST_NRAS_SIGNALING_DN	68	0.29	2.85	0.000	0.000	0.012	2984	tags=57%, list=28%, signal=80%
50	FISCHER_G1_S_CELL_CYCLE	146	0.20	2.83	0.000	0.000	0.015	3211	tags=51%, list=30%, signal=72%

ALL_DOWN after TP-3654_top 50

	GS	**SIZE**	**ES**	**NES**	**NOM p-val**	**FDR q-val**	**FWER p-val**	**RANK AT MAX**	**LEADING EDGE**
1	PENG_GLUTAMINE_DEPRIVATION_DN	294	-0.51	-9.84	0.000	0.000	0.000	2245	tags=70%, list=21%, signal=87%
2	PENG_RAPAMYCIN_RESPONSE_DN	217	-0.48	-8.18	0.000	0.000	0.000	2244	tags=68%, list=21%, signal=85%
3	PENG_LEUCINE_DEPRIVATION_DN	172	-0.47	-7.10	0.000	0.000	0.000	2155	tags=66%, list=20%, signal=82%
4	GARY_CD5_TARGETS_DN	389	-0.31	-7.05	0.000	0.000	0.000	2283	tags=51%, list=22%, signal=63%
5	MANALO_HYPOXIA_DN	248	-0.39	-7.01	0.000	0.000	0.000	2667	tags=63%, list=25%, signal=83%
6	MOOTHA_MITOCHONDRIA	362	-0.30	-6.53	0.000	0.000	0.000	2685	tags=55%, list=25%, signal=71%
7	TIEN_INTESTINE_PROBIOTICS_24HR_UP	490	-0.25	-6.45	0.000	0.000	0.000	2475	tags=48%, list=24%, signal=59%
8	WONG_MITOCHONDRIA_GENE_MODULE	197	-0.41	-6.42	0.000	0.000	0.000	2385	tags=62%, list=23%, signal=79%
9	MOOTHA_HUMAN_MITODB_6_2002	355	-0.28	-6.02	0.000	0.000	0.000	2121	tags=48%, list=20%, signal=58%
10	STARK_PREFRONTAL_CORTEX_22Q11_DELETION_DN	404	-0.25	-5.81	0.000	0.000	0.000	2385	tags=47%, list=23%, signal=58%
11	YAO_TEMPORAL_RES	114	-0.46	-5.76	0.000	0.000	0.000	3113	tags=75%,

	PONSE_TO_PROGESTERONE_CLUSTER_14								list=30%, signal=105%
12	KEGG_PROTEASOME	40	-0.74	-5.63	0.000	0.000	0.000	1683	tags=90%, list=16%, signal=107%
13	TARTE_PLASMA_CELL_VS_PLASMABLAST_DN	282	-0.29	-5.62	0.000	0.000	0.000	2257	tags=49%, list=21%, signal=61%
14	YAO_TEMPORAL_RESPONSE_TO_PROGESTERONE_CLUSTER_11	80	-0.54	-5.56	0.000	0.000	0.000	2101	tags=74%, list=20%, signal=91%
15	YAO_TEMPORAL_RESPONSE_TO_PROGESTERONE_CLUSTER_17	151	-0.38	-5.38	0.000	0.000	0.000	2307	tags=59%, list=22%, signal=74%
16	SCHLOSSER_MYC_TARGETS_REPRESSED_BY_SERUM	148	-0.38	-5.36	0.000	0.000	0.000	2916	tags=66%, list=28%, signal=89%
17	SCHLOSSER_MYC_TARGETS_AND_SERUM_RESPONSE_DN	44	-0.67	-5.26	0.000	0.000	0.000	1549	tags=82%, list=15%, signal=96%
18	GRADE_COLON_AND_RECTAL_CANCER_UP	232	-0.29	-5.22	0.000	0.000	0.000	2161	tags=49%, list=21%, signal=60%
19	SCHUHMACHER_MYC_TARGETS_UP	65	-0.55	-5.21	0.000	0.000	0.000	1098	tags=65%, list=10%, signal=72%
20	REACTOME_TCA_CYCLE_AND_RESPIRATORY_ELECTRON_TRANSPORT	110	-0.42	-5.20	0.000	0.000	0.000	2667	tags=67%, list=25%, signal=89%
21	ELVIDGE_HYPOXIA_DN	120	-0.40	-5.14	0.000	0.000	0.000	2730	tags=66%, list=26%, signal=88%
22	YAO_TEMPORAL_RESPONSE_TO_PROGESTERONE_CLUSTER_13	152	-0.36	-5.13	0.000	0.000	0.000	2673	tags=61%, list=25%, signal=80%
23	REACTOME_REGULATION_OF_ORNITHINE_DECARBOXYLASE_ODC	45	-0.63	-5.00	0.000	0.000	0.000	1805	tags=80%, list=17%, signal=96%
24	REACTOME_CROSS_PRESENTATION_OF_SOLUBLE_EXOGENOUS_ANTIGENS_ENDOSOMES	42	-0.64	-4.94	0.000	0.000	0.000	1805	tags=81%, list=17%, signal=97%
25	REACTOME_ER_PHAGOSOME_PATHWAY	54	-0.55	-4.93	0.000	0.000	0.000	1805	tags=72%, list=17%, signal=87%
26	REACTOME_CDK_MEDIATED_PHOSPHORYLATION_AND_REMOVAL_OF_CDC6	44	-0.63	-4.93	0.000	0.000	0.000	1805	tags=80%, list=17%, signal=96%
27	REACTOME_DESTABILIZATION_OF_MRNA_BY_AUF1_HNRNP_D0	48	-0.60	-4.92	0.000	0.000	0.000	1805	tags=77%, list=17%, signal=93%

28	REACTOME_METABOLISM_OF_AMINO_ACIDS_AND_DERIVATIVES	111	-0.40	-4.86	0.000	0.000	0.000	1805	tags=57%, list=17%, signal=68%
29	CHANG_CORE_SERUM_RESPONSE_UP	178	-0.31	-4.85	0.000	0.000	0.000	1665	tags=46%, list=16%, signal=54%
30	KARLSSON_TGFB1_TARGETS_UP	103	-0.41	-4.80	0.000	0.000	0.000	1782	tags=57%, list=17%, signal=68%
31	REACTOME_AUTODEGRADATION_OF_THE_E3_UBIQUITIN_LIGASE_COP1	45	-0.61	-4.78	0.000	0.000	0.000	1805	tags=78%, list=17%, signal=93%
32	REACTOME_VIF_MEDIATED_DEGRADATION_OF_APOBEC3G	47	-0.60	-4.76	0.000	0.000	0.000	1805	tags=77%, list=17%, signal=92%
33	REACTOME_P53_INDEPENDENT_G1_S_DNA_DAMAGE_CHECKPOINT	46	-0.59	-4.74	0.000	0.000	0.000	1805	tags=76%, list=17%, signal=91%
34	REACTOME_SCF_BETA_TRCP_MEDIATED_DEGRADATION_OF_EMI1	47	-0.58	-4.72	0.000	0.000	0.000	1810	tags=74%, list=17%, signal=90%
35	WONG_EMBRYONIC_STEM_CELL_CORE	304	-0.24	-4.71	0.000	0.000	0.000	1986	tags=42%, list=19%, signal=51%
36	BIOCARTA_PROTEASOME_PATHWAY	28	-0.75	-4.70	0.000	0.000	0.000	1917	tags=93%, list=18%, signal=113%
37	KEGG_OXIDATIVE_PHOSPHORYLATION	97	-0.40	-4.67	0.000	0.000	0.000	2525	tags=64%, list=24%, signal=83%
38	KEGG_PARKINSONS_DISEASE	89	-0.42	-4.60	0.000	0.000	0.000	2525	tags=65%, list=24%, signal=85%
39	REACTOME_REGULATION_OF_MRNA_STABILITY_BY_PROTEINS_THAT_BIND_AU_RICH_ELEMENTS	78	-0.44	-4.57	0.000	0.000	0.000	2730	tags=69%, list=26%, signal=93%
40	HORTON_SREBF_TARGETS	19	-0.85	-4.53	0.000	0.000	0.000	1571	tags=100%, list=15%, signal=117%
41	REACTOME_RESPIRATORY_ELECTRON_TRANSPORT_ATP_SYNTHESIS_BY_CHEMIOSMOTIC_COUPLING_AND_HEAT_PRODUCTION_BY_UNCOUPLING_PROTEINS_	77	-0.44	-4.52	0.000	0.000	0.000	2525	tags=68%, list=24%, signal=88%
42	REACTOME_AUTODEGRADATION_OF_CDH1_BY_CDH1_APC_C	53	-0.51	-4.52	0.000	0.000	0.000	1805	tags=68%, list=17%, signal=82%

43	MOOTHA_PGC	320	-0.22	-4.50	0.000	0.000	0.000	2782	tags=48%, list=26%, signal=63%
44	REACTOME_P53_DEPENDENT_G1_DNA_DAMAGE_RESPONSE	51	-0.52	-4.44	0.000	0.000	0.000	1805	tags=69%, list=17%, signal=82%
45	REACTOME_REGULATION_OF_APOPTOSIS	50	-0.53	-4.42	0.000	0.000	0.000	1805	tags=70%, list=17%, signal=84%
46	REACTOME_ANTIGEN_PROCESSING_CROSS_PRESENTATION	61	-0.49	-4.39	0.000	0.000	0.000	1805	tags=66%, list=17%, signal=79%
47	BERENJENO_TRANSFORMED_BY_RHOA_UP	440	-0.19	-4.35	0.000	0.000	0.000	1665	tags=34%, list=16%, signal=38%
48	REACTOME_CDT1_ASSOCIATION_WITH_THE_CDC6_ORC_ORIGIN_COMPLEX	52	-0.50	-4.30	0.000	0.000	0.000	1805	tags=67%, list=17%, signal=81%
49	SCHLOSSER_MYC_TARGETS_AND_SERUM_RESPONSE_UP	45	-0.54	-4.28	0.000	0.000	0.000	2303	tags=76%, list=22%, signal=96%
50	BOYAULT_LIVER_CANCER_SUBCLASS_G3_UP	169	-0.28	-4.27	0.000	0.000	0.000	2552	tags=52%, list=24%, signal=68%

Figure S1

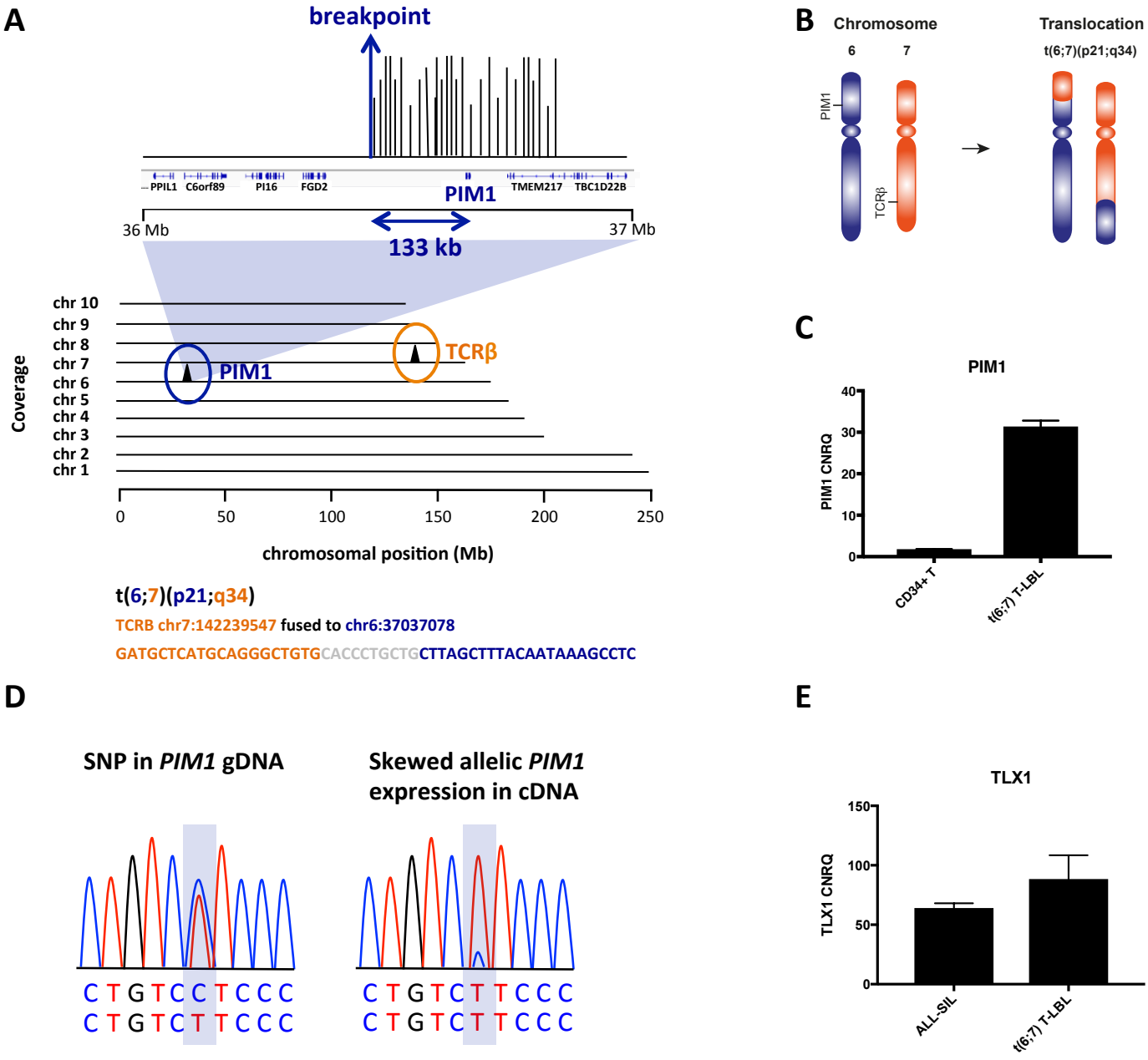
A
breakpoint
PPIL1
C6orf89
PI16
FGD2
PIM1
TMEM217
TBC1D22B
36 Mb
37 Mb
133 kb
chr 10
chr 9
chr 8
chr 7
chr 6
chr 5
chr 4
chr 3
chr 2
chr 1
Coverage
PIM1
TCRβ
0
50
100
150
200
250
chromosomal position (Mb)
t(6;7)(p21;q34)
TCRB chr7:142239547 fused to chr6:37037078
GATGCTCATGCAGGGCTGTGCACCCTGCTGCTTAGCTTTACAATAAAGCCTC
B
Chromosome
Translocation
6
7
t(6;7)(p21;q34)
PIM1
TCRβ
C
PIM1
PIM1 CNRQ
40
30
20
10
0
CD34+ T
t(6;7) T-LBL
D
SNP in PIM1 gDNA
Skewed allelic PIM1 expression in cDNA
C T G T C C T C C C
C T G T C T T C C C
C T G T C T T C C C
C T G T C T T C C C
E
TLX1
TLX1 CNRQ
150
100
50
0
ALL-SIL
t(6;7) T-LBL

Figure S2

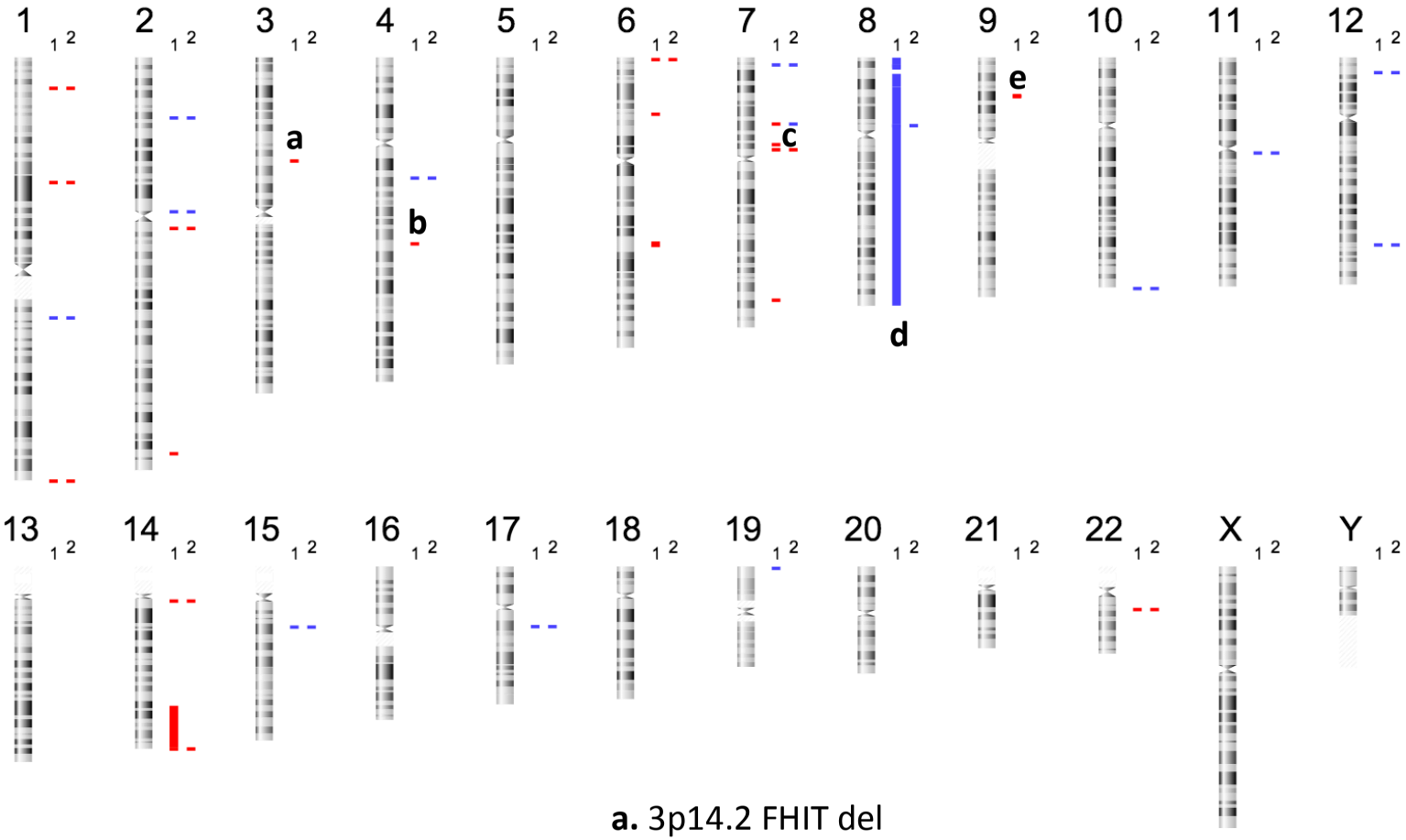

1: pleural effusion
2: bone marrow

red = loss
blue = gain

a. 3p14.2 FHIT del

b. 4q25 LEF1 del

c. 7p12.1 IKZF1 del

d. trisomy chr 8

e. 9p21 CDKN2A del

Figure S3

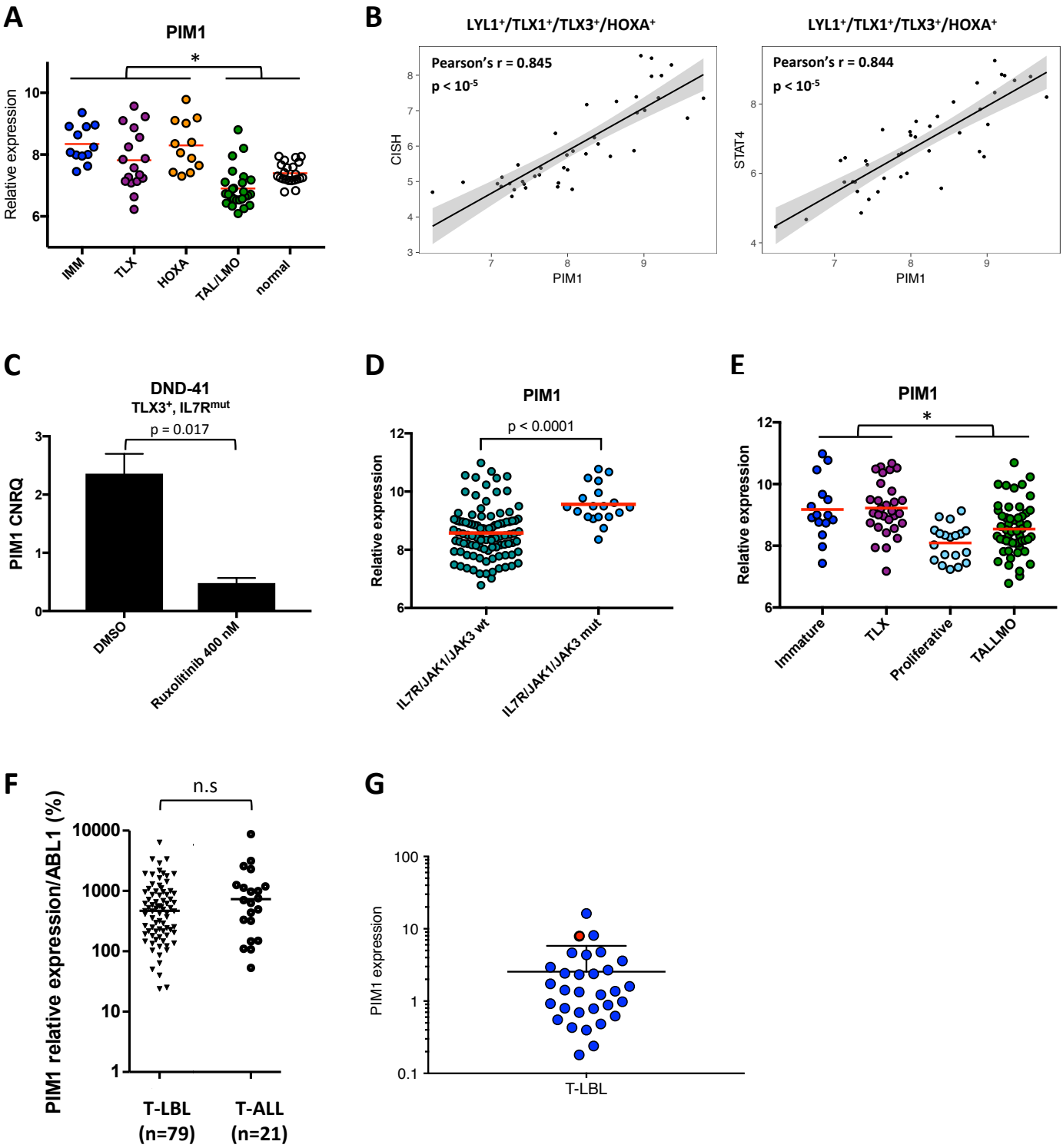
A
PIM1
*
Relative expression
10
8
6
IMM
TLX
HOXA
TAL/LMO
normal
B
LYL1+/TLX1+/TLX3+/HOXA+
Pearson's r = 0.845
p < 10-5
CISH
PIM1
LYL1+/TLX1+/TLX3+/HOXA+
Pearson's r = 0.844
p < 10-5
STAT4
PIM1
C
DND-41
TLX3+, IL7Rmut
p = 0.017
PIM1 CNRQ
DMSO
Ruxolitinib 400 nM
D
PIM1
p < 0.0001
Relative expression
IL7R/JAK1/JAK3 wt
IL7R/JAK1/JAK3 mut
E
PIM1
*
Relative expression
Immature
TLX
Proliferative
TALLMO
F
n.s
PIM1 relative expression/ABL1 (%)
10000
1000
100
10
1
T-LBL (n=79)
T-ALL (n=21)
G
PIM1 expression
100
10
1
0.1
T-LBL

Figure S4

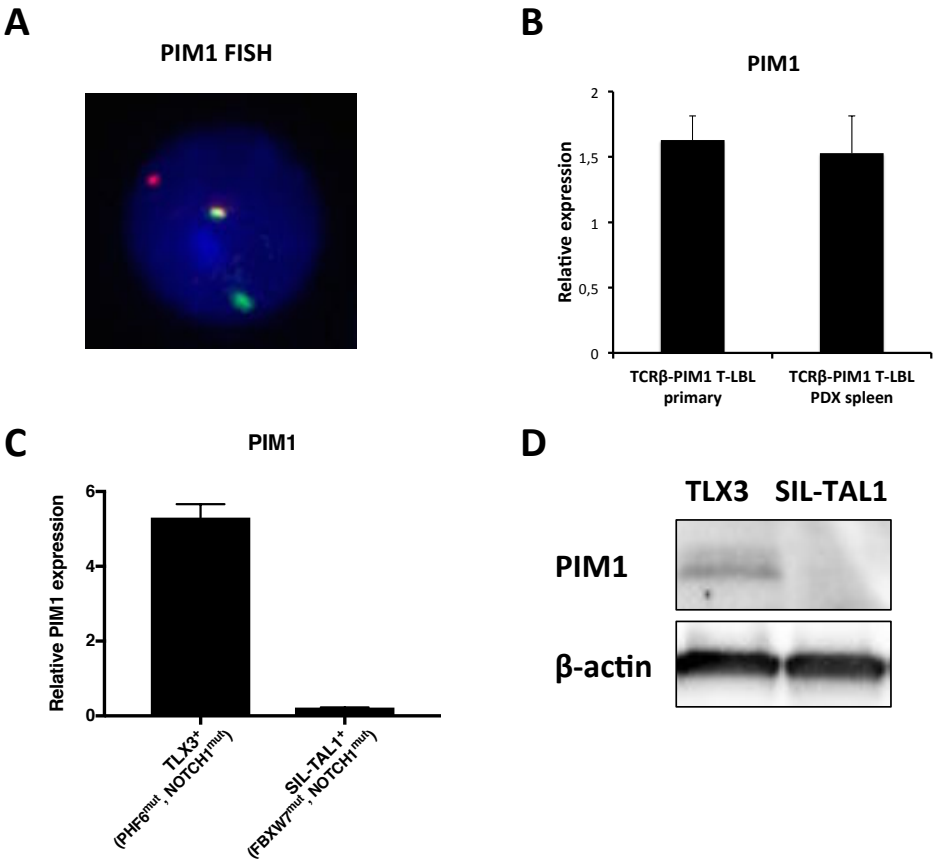

Figure S5

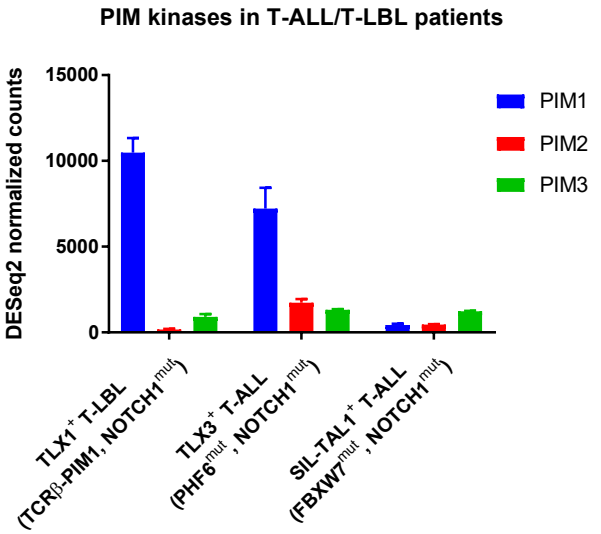

Figure S6

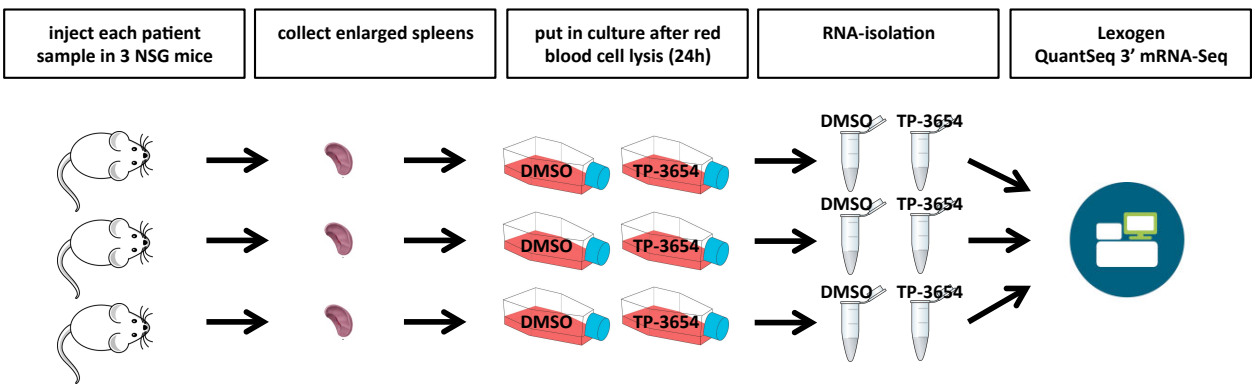

Figure S7

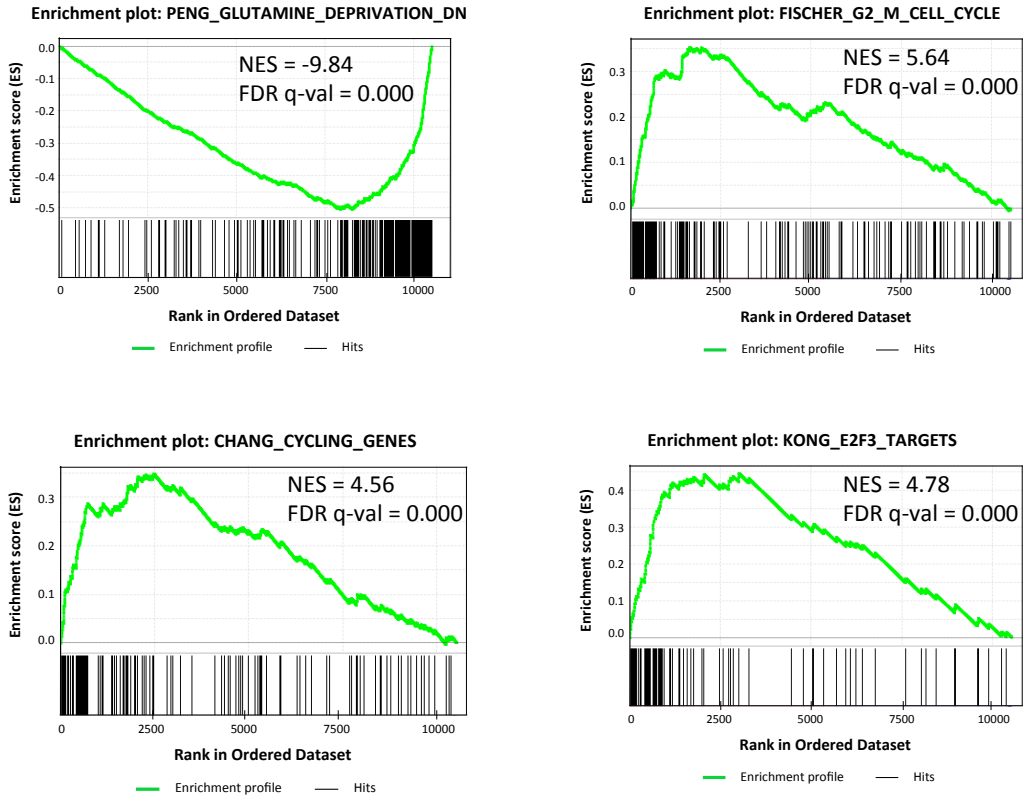

Figure S8

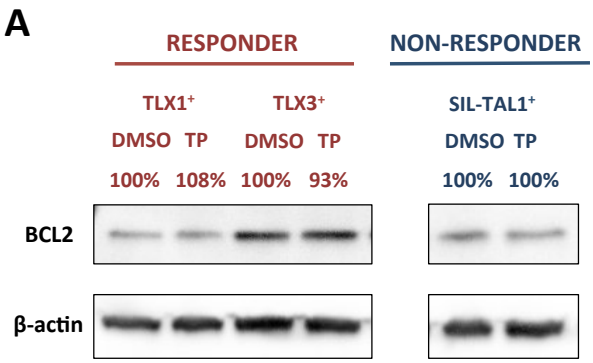

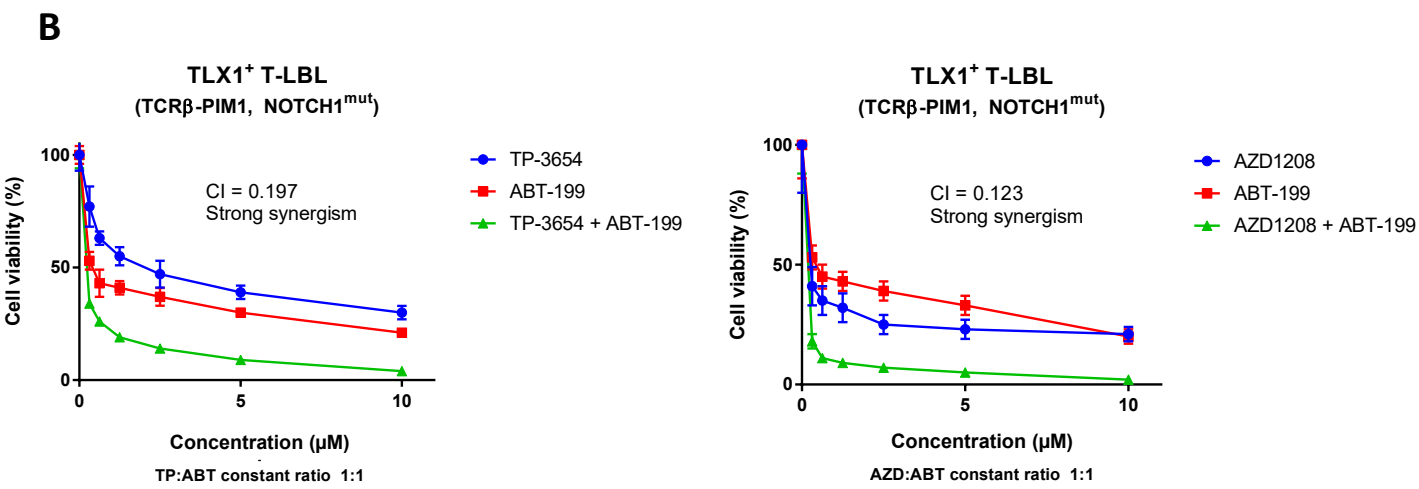

Figure S9

A

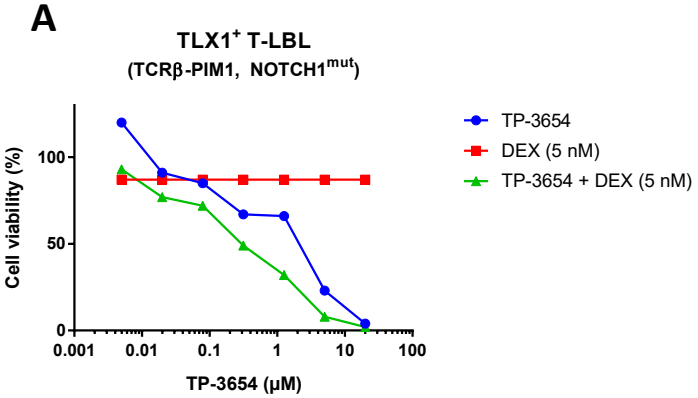

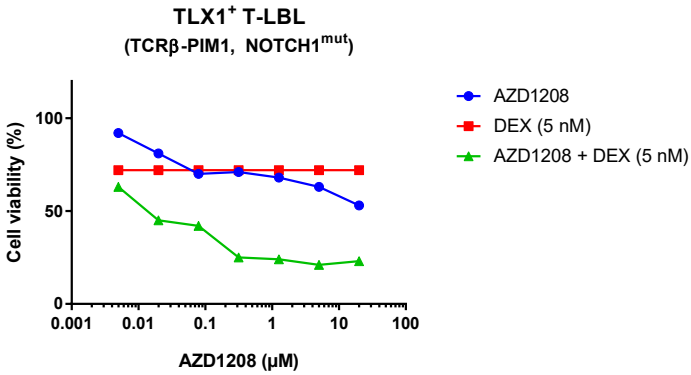

B

TCRβ-PIM1 TLX1+ PIM1high T-LBL

TP-3654 and dexamethasone

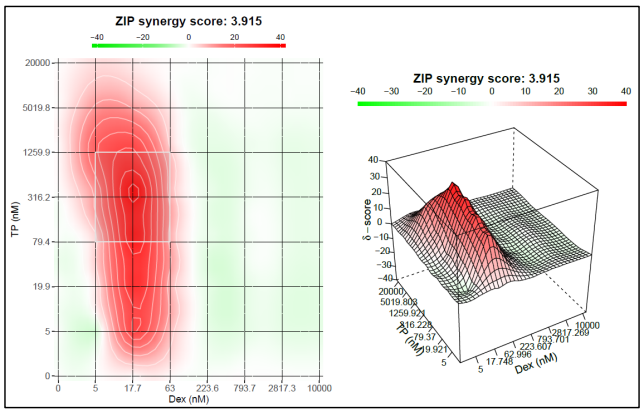

Synergy score	3,92
Most synergistic area score	16,33
Method	ZIP

AZD1208 and dexamethasone

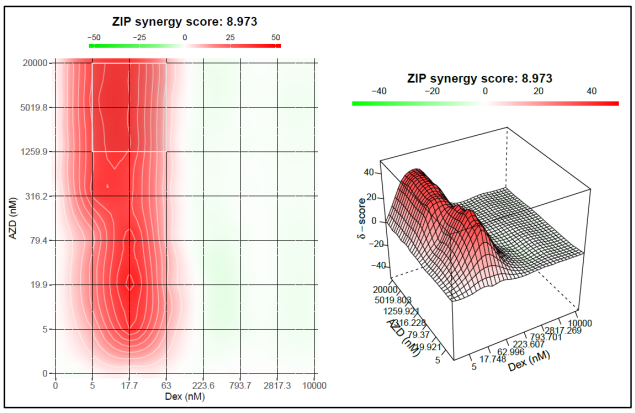

Synergy score	9,97
Most synergistic area score	24,23
Method	ZIP

https://synergyfinder.fimm.fi/

SUPPLEMENTARY METHODS

Targeted Locus Amplification (TLA)

Preparation of the samples for TLA was performed as described (1). In brief, cells were crosslinked using formaldehyde and DNA was digested with NlaIII. The samples were ligated, crosslinks reversed, and the DNA purified. To obtain circular chimeric DNA molecules for PCR amplification, the DNA molecules were trimmed with NspI and ligated at a DNA concentration of 5 ng/µl to promote intramolecular ligation. Importantly, NspI was chosen for its RCATGY recognition sequence that encompasses the CATG recognition sequence of NlaIII. As a consequence, only a subset of NlaIII (CATG) sites were (re-)digested, generating DNA fragments of approximately 2 kb and allowing the amplification of entire restriction fragments. Sequences of the TCRB primers are (5 to 3): TCRB_F TAGTCTTAACACCTCCAGCT and TCRB_R TAGCCTATTTCGTACTTGGG. After ligation, the DNA was purified, and PCR products were purified and library prepped using the Illumina NexteraXT protocol and sequenced on an Illumina Miseq sequencer. Reads were mapped using BWA-SW, which is a Smith-Waterman alignment tool. This allows partial mapping, which is optimally suited for identifying break-spanning reads. The human genome version hg19 was used for mapping.

Cell lines and patient samples

Cell lines were purchased from the DSMZ repository (Braunschweig, Germany) and cultured in RPMI 1640 medium supplemented with 10% fetal bovine serum (FBS), 100 U/mL penicillin, 100 mg/mL streptomycin, 100 mg/mL kanamycin sulfate, and 2 mM L-glutamine at 37°C with 5% CO2. Primary T-ALL cells for *in vitro* TP-3654, AZD1208 and dexamethasone treatment and xenograft studies were acquired by informed consent from the Department of Pediatric Hematology-Oncology at Ghent University Hospital and Leuven University Hospital. These primary T-ALL samples were assigned to a specific molecular genetic subclass based on real-time polymerase chain reaction of *SIL-TAL1*, *TLX1* or *TLX3*. Primary T-ALL and T-LBL cells for *PIM1* qPCR analysis were acquired by informed consent from the Department of Hematology at the Necker-Enfants Malades Hospital, Paris, France and from Padova Hospital, Italy. The TCRβ-PIM1 positive case described in this study was a 5 year old female that was diagnosed with T-LBL and treated according to EORTC 58951. In that treatment protocol, she was allocated to the average risk 2 (AR2) group. She had a good initial steroid response and is currently still in 1st complete remission (CR).

Quantitative real-time polymerase chain reactions

Total RNA was isolated using the miRNeasy mini kit (Qiagen) and the RNAse-Free Dnase set (Qiagen).

The iScript cDNA synthesis kit (Bio-Rad) was used to synthesize cDNA. The quantitative real-time polymerase chain reactions were performed using the SsoAdvanced SYBR Green Supermix (Bio-Rad) and were run on the LightCycler480 (Roche, model LC480). Every sample was analyzed in duplicate and the gene expression was standardized against at least 3 housekeeping genes. The primer sequences used are (5' to 3'):

PIM1_F CGAGCATGACGAAGAGATCAT and PIM1_R TCGAAGGTTGGCCTATCTGA, TLX1_F AACGTGGGATTCAGAGAAAG and TLX1_R CCATGTGTGTGATGAGAAGT, HMBS_F GGCAATGCGGCTGCAA and HMBS_R GGGTACCCACGCGAATCAC, TBP_F CACGAACCACGGCACTGATT and TBP_R TTTTCTTGCTGCCAGTCTGGAC, B2M_F GCTGTCTCCATGTTTGATGTATCT and B2M_R TCTCTGCTCCCCACCTCTAAGT, HPRT1_F TGACACTGGCAAAACAATGCA and HPRT1_R GGTCCTTTTCACCAGCAAGCT, UBC_F ATTTGGGTCGCGGTTCTTG and UBC_R TGCCTTGACATTCTCGATGGT.

Western blotting

Cells were lysed with radioimmunoprecipitation assay (RIPA) buffer and protein concentration was measured with the Pierce BCA protein assay kit. Denatured protein was loaded on a 10% polyacrylamide gel and the sodium dodecyl sulfate-polyacrylamide gel electrophoresis was run followed by western blotting on a nitrocellulose membrane. The primary antibodies used were: PIM1 (#2907, Cell Signaling Technology, 1:1000), c-Myc Ser62 (#13748, Cell Signaling Technology, 1:1000), c-Myc total (sc-764, Santa Cruz Biotechnology, 1:1000), p70S6K Thr389 (#9205, Cell Signaling Technology, 1:1000), p70S6K total (#9202, Cell Signaling Technology, 1:1000), MCL1 (#5453, Cell Signaling Technology, 1:1000), β-actin (Clone AC-75; A2228; Sigma-Aldrich; dilution 1:10000). The protein bands were densitometric analyzed using ImageJ software (National Institutes of Health).

***In vitro* drug profiling on xenograft T-ALL and T-LBL samples**

Drug responses were assessed in T-ALL/T-LBL cell co-cultures on hTERT-immortalized primary bone marrow mesenchymal stromal cells (MSC) (2) as described (3) in 384-well plates (Greiner, REF781090). $2.5x10^3$ MSC cells/well were plated in 30µL AIM-V® medium 24h before adding $2\text{-}3x10^4$ T-ALL cells in 27.5µL medium recovered from cryopreserved samples. Compounds were reconstituted in DMSO (10mM stock concentrations) and stored at -80°C. Serially-diluted drugs were prepared using epMotion 5070 and Tecan D300 robots.

In vivo treatment of xenografts with PIM inhibitors and dexamethasone

Nonobese diabetic/severe combined immunodeficient γ (NSG) mice were injected tail vein at 6 weeks of age with 150µL phosphate-buffered saline containing 2.5×10^6 human T-LBL pleural

effusion cells. At regular time points, leukemia engraftment was monitored by human CD45 staining (CD45-FITC antibody; Miltenyi Biotec) in peripheral blood using flowcytometry analysis. Upon establishment of disease, human leukemic cells were isolated from the spleen and retransplanted into secondary recipients. At 4 to 5 weeks, the cells were engrafted and the mice were randomly divided into 4 groups and treatment was started. Mice were treated with 125 mg TP-3654/kg body weight or with 30 mg AZD1208 mg/kg body weight or with vehicle via oral gavage for 3 weeks (5 days on, 2 days off). TP-3654 was formulated in 10% TWEEN-20 (Sigma-Aldrich) in water, AZD1208 was formulated in 10% DMSO, 45% PEG400 (Sigma-Aldrich) and 45% methylcellulose (0.5% stock solution. Percentage human CD45-positive (%hCD45) cells in the peripheral blood was weekly measured. After treatment, animals were sacrificed and the spleen weight and %hCD45-positive leukemic blasts in bone marrow and spleen were determined by flowcytometry as described above.

For combination therapy with TP-3654 and dexamethasone tertiary xenograft injections were performed in a cohort of 24 NSG mice. Upon detection of human CD45 leukemic blasts in peripheral blood, mice were randomized in 4 groups and treated with vehicle, 125 mg TP-3654/kg body weight via oral gavage, 5 mg dexamethasone/kg body weight via i.p. or both TP-3654 and dexamethasone at same concentrations used in the monotherapy groups. Dexamethasone (Aacidexam) was formulated in 100% phosphate-buffered saline. Mice were treated for 3 weeks (5 days on, 2 days off) and %hCD45 in peripheral blood was followed weekly. After treatment we monitored survival of the mice by means of 'human ethical endpoints', where mice were sacrificed when they suffered from more than 20% weight loss, or more than 65% leukemic blasts in the peripheral blood.

Additional T-ALL patient samples were injected for short term TP-3654 treatment. For each patient 6 NSG mice were injected tail vein with 2.5 million patient cells. Upon engraftment treatment was started with vehicle or 125 mg TP-3654/kg body weight for 5 consecutive days. %hCD45 in peripheral blood was determined at the first and last day of treatment. Upon establishment of full-blown leukemia, vehicle mice were sacrificed, spleens were processed and red blood cells lysed. Cells were put in culture in RPMI 1640 medium supplemented with 10% FBS and treated with 1 µM AZD1208 or 1 µM TP-3654. DMSO was used as a control. Cells were collected after 6 hours for protein extraction and after 24 hours for RNA extraction. RNA samples were subsequently prepared for QuantSeq 3' mRNA sequencing (Lexogen).

The ethical committee on animal welfare at Ghent University Hospital approved all animal experiments.

QuantSeq 3' mRNA sequencing

Total RNA samples (500 ng) were cleaned using DNAse I kit according to the Rapid out removal DNA kit instruction (Thermoscientific) and converted into cDNA by using QuantSeq 3' mRNA-seq reverse

Library Prep Kit (Lexogen) according to manufacturer's instruction (4) to generate compatible library for Illumina sequencing. Briefly, library generation was initiated by oligodT priming for first strand cDNA which generated one fragment per transcript. The second strand cDNA was subsequently synthesised using random primers. Illumina-specific linker sequences were introduced by the primer with barcoding indices for different samples. The quality of cDNA libraries was determined using a High Sensitivity DNA Assay 2100 Bioanalyzer (Agilent) for quality control analysis. Sequencing of the cDNA library with 75 bp single end reads was performed using an Illumina HiSeq 2500 system.

Reads were aligned to the reference genome GRCh38 using STAR-2.4.2a with default settings (5). STAR was also used for gene expression quantification on the Ensembl GTF file version 84. Differential expression analysis was performed using DESeq2 in R (6). A paired design was implemented comparing drug treated samples to DMSO with reference to the mice the samples originated from.

Statistical analysis

GraphPad Prism 7.0 (La Jolla, CA) was used for statistical analyses. The Mann-Whitney *U* test was used to analyze differences between groups. Data were considered statistically significant for *P* values less than .05. Pearson correlation analysis of microarray data was performed in R software.

REFERENCES

1. de Vree PJ, de Wit E, Yilmaz M et al. Targeted sequencing by proximity ligation for comprehensive variant detection and local haplotyping. Nat Biotechnol. 2014 Oct;32(10):1019-25.
2. Mihara K, Imai C, Coustan-Smith E et al. Development and functional characterization of human bone marrow mesenchymal cells immortalized by enforced expression of telomerase. Br J Haematol. 2003 Mar;120(5):846-9.
3. Bonapace L, Bornhauser BC, Schmitz M et al. Induction of autophagy-dependent necroptosis is required for childhood acute lymphoblastic leukemia cells to overcome glucocorticoid resistance. J Clin Invest. 2010 Apr;120(4):1310-23.
4. Moll P, Ante M, Seitz A, Reda T. QuantSeq 3′ mRNA sequencing for RNA quantification. Nature Methods. 2014;11(12).
5. Dobin A, Davis CA, Schlesinger F et al. STAR: ultrafast universal RNA-seq aligner. Bioinformatics. 2013 Jan 1;29(1):15-21.
6. Love MI, Huber W, Anders S. Moderated estimation of fold change and dispersion for RNA-seq data with DESeq2. Genome Biol. 2014;15(12):550.